The Journal of Molecular Diagnostics, Vol. 16, No. 6, November 2014

the Journal of Molecular Diagnostics
jmd.amjpathol.org

See related Commentary on page 612

# Seven Novel Probe Systems for Real-Time PCR Provide Absolute Single-Base Discrimination, Higher Signaling, and Generic Components

James L. Murray,* Peixu Hu,*† and David A. Shafer*†

*From GeneTAG Technology, Inc.,* Atlanta, Georgia; and the Department of Psychiatry and Behavioral Sciences,† Emory University School of Medicine, Atlanta, Georgia*

Accepted for publication June 11, 2014.

Address correspondence to David A. Shafer, Ph.D., GeneTAG Technology, Inc., 3781 Presidential Pkwy., Ste. 9, Atlanta, GA 30340. E-mail: dshafer@genetagtechnology.com.

We have developed novel probe systems for real-time PCR that provide higher specificity, greater sensitivity, and lower cost relative to dual-labeled probes. The seven DNA Detection Switch (DDS)-probe systems reported here employ two interacting polynucleotide components: a fluorescently labeled probe and a quencher antiprobe. High-fidelity detection is achieved with three DDS designs: two internal probes (internal DDS and Flip probes) and a primer probe (ZIPR probe), wherein each probe is combined with a carefully engineered, slightly mismatched, error-checking antiprobe. The antiprobe blocks off-target detection over a wide range of temperatures and facilitates multiplexing. Other designs (Universal probe, Half-Universal probe, and MacMan probe) use generic components that enable low-cost detection. Finally, single-molecule G-Force probes employ guanine-mediated fluorescent quenching by forming a hairpin between adjacent C-rich and G-rich sequences. Examples provided show how these probe technologies discriminate drug-resistant *Mycobacterium tuberculosis* mutants, *Escherichia coli* O157:H7, oncogenic *EGFR* deletion mutations, hepatitis B virus, influenza A/B strains, and single-nucleotide polymorphisms in the human *VKORC1* gene. *(J Mol Diagn 2014, 16: 627—638; http://dx.doi.org/10.1016/j.jmoldx.2014.06.008)*

Quantitative real-time PCR (qPCR) assays are typically based on TaqMan or Molecular Beacon probes that mechanistically require amplification of a target region using a pair of flanking primers, and fluorescent detection of an internal sequence with a dual-labeled probe, generally having a 5′ fluorophore and a 3′ quencher.[1,2] The typical cost of such probes is around US $150 to $250 per target, due to the special costs of making and purifying dual-labeled probes. Floating TaqMan probes are quenched in the absence of targets due to random coiling in solution, which allows their fluor- and quencher-labeled ends to come together. TaqMan fluorescence occurs when the probe binds to the target and the advancing Taq polymerase then cleaves the fluorophore from the probe.[3] In contrast, Molecular Beacon probes are designed with a set of 5 to 7 matching bases on their 5′ and 3′ ends, which induce hairpin formation and stabilize the quenched state.[2] Fluorescent detection results when such probes hybridize with their targets and the labeled ends are separated.

Although TaqMan and Molecular Beacon probes are reliable for detecting matching target sequences, they can be more difficult to design and less effective when discriminating between closely related targets, especially single-nucleotide polymorphisms (SNPs), drug-resistant mutants, or somatic cancer mutations.[4,5] In these situations, an effective probe requires a careful balancing act based on melting temperature ($T_m$) so that the probe correctly touches down and positively detects a fully matching target at an optimized annealing temperature, while at that same temperature, it does not bind or detect similar targets differing by a single base. Thus, repeated design and testing are commonly

Supported by Small Business Innovative Research grants from the NIH (1R43AI081511 and 1R43AI090852 to D.A.S./GeneTAG).

Disclosures: D.A.S. is the President, Founder, and principal shareholder of GeneTAG Technology, Inc. P.H. is the Vice President and a shareholder of GeneTAG Technology. J.L.M. is an employee of GeneTAG Technology. These technologies are covered by US patent no. 8,076,067 and other patents pending.


http://dx.doi.org/10.1016/j.jmoldx.2014.06.008

**Table 1** Sequences of Primers, Probes, and Antiprobes Used in This Study

| Target organism | Target gene | Primer, probe, or antiprobe sequence |
|---|---|---|
| *E. coli* | O157:H7 *uidA* | Fwd: 5′-CAGTCTGGATCGCGAAAACTG-3′ |
| | | Rev: 5′-ACCAGACGTTGCCCACATAATT-3′ |
| | | TaqMan MGB P: 5′-TET-ATTGAGCAGCGTTGG-MGB/NFQ-3′ |
| | | iDDS P: 5′-FAM-CACCAACGCTGCTCAATTC-Phos-3′ |
| | | iDDS AP: 5′-GAATTGAGC**T**GCGTTGGTG-BHQ1-3′ |
| Hepatitis B | *S* | Fwd: 5′-GTGTCTGCGGCGTTTTATCA-3′ |
| | | Rev: 5′-GACAAACGGGCAACATACCTT-3′ |
| | | MacMan P: 5′-CAL Fluor Red 610-CCTCTKCATCCTGCTGCTATGCCTCATC-CCCCTCCTTCTCTCC-3′ |
| | | MacMan AP: 5′-GA+GAA+GGA+GG+GG-BHQ2-3′ |
| | | TaqMan P: 5′-CAL Fluor Red 610-CCTCTKCATCCTGCTGCTATGCCTCATC-BHQ2-3′ |
| Human | *EGFR* deletion mutant in exon 19 (d-19) | Fwd. ZIPR P: 5′-CAL Fluor Red 610-TCTGGATCCCAGAAGGTGAG-3′ |
| | | ZIPR AP: 5′-CTCACCTTCTGGG**T**TCCAGA-BHQ2-3′ |
| | | Rev: 5′-CGTAGGCTTCATCGAGGATT-3′ |
| | | iDDS P: 5′-FAM-CAAGGAATTAAGAGAAGCAACATC-Phos-3′ |
| | | iDDS AP: 5′-GATGTTGC**C**TCTCTTAATTCCTTG-BHQ1-3′ |
| Human | *VKORC1* | Fwd. G-Force P: 5′-FAM-CCCCTCCA-S18-AGGAGGGGGCCTCTGGGAAGTCA-AGCAAG-3′ |
| | | Rev: 5′-AAATGCTAGGATTATAGGCGTGA-3′ |
| Human | *VKORC1* SNP *rs9923231*[C] | Fwd: 5′-CCTCTGGGAAGTCAAGCAAG-3′ |
| | | Rev: 5′-AAATGCTAGGATTATAGGCGTGA-3′ |
| | | iDDS P: 5′-FAM-CGCACCCGGCCAATG-Phos-3′ |
| | | iDDS AP: 5′-CAT**C**GGCCGGGTGCG-BHQ1-3′ |
| Influenza A | A/California/04/2009 *HA1*, target #1 | Fwd: 5′-GTAGTTCTGCTATATACATTTGCAACC-3′ |
| | | Rev LP: 5′-GCTACGTAGACTAGACGTTCCCTATACATAATGTGTCTGCATTTG-3′ |
| | | UP: 5′-FAM-CCCTATCGCTACGTAGACTAGACGTTC-3′ |
| | | UAP: 5′-TAGTCTACGTAGCGATAGGG-BHQ1-3′ |
| | A/California/4/2009 *HA1*, target #2 | Fwd. HUP: 5′-FAM-CGTAGACTAGACGTTCGTGAATCACTCTCCACAGCAAG-3′ |
| | | HUAP: 5′-GAACGTCTAGTCTA-BHQ1-3′ |
| | | Rev: 5′-GTAACACGTTCCATTGTCTGAAC-3′ |
| | A/California/4/2009 *HA1*, target #3 | Fwd: 5′-GGCAATACTAGTAGTTCTGCTATAT-3′ |
| | | Rev. HUP: 5′-Quasar 670-GCACGCTACGTACTAGGTAATGTGTCTGCAT-TTGCGGT-3′ |
| | | HUAP: 5′-CCTAGTACGTAGCGTGC-BHQ2-3′ |
| | A/California/4/2009 *HA1*, target #4 | Fwd: 5′-GTGCTATAAACACCAGCCTYCCA-3′ |
| | | Rev: 5′-CGGGATATTCCTTAATCCTGTRGC-3′ |
| | | TaqMan P: 5′-FAM-CAGAATATACA-BHQ1-CCRGTCACAATTGGARAA-S3-3′ |
| | A/California/4/2009 *HA1*, target #5 | Fwd: 5′-ATTTAATATGGCTAGTTAAAAAAGGAAA-3′ |
| | | Rev. HUP: 5′-HEX-CATAGGTACCCTACGGACTTCTTTCCCTTTATCATTAATG-3′ |
| | | HUAP: 5′-GTAGGGTACCTATG-BHQ2-3′ |
| | A/California/4/2009 *HA1*, target #6 | Fwd: 5′-TTCGCAATGGAAAGAAATGC-3′ |
| | | Rev. HUP: 5′-CAL Fluor Red 610-ACGCCTAAGAGTAGCAAGTTGTATTGCA-ATCGTGG-3′ |
| | | HUAP: 5′-CTACTCTTAGGCGT-BHQ2-3′ |
| Influenza A | A/Fujian/411/02 *HA3*, target #1 | Fwd LP: 5′-GCTACGTAGACTAGACGTTCCCTTTTTGTTGAACGCAGCA-3′ |
| | | Rev: 5′-CTAGTGACCTAAGGGAGGCATAATC-3′ |
| | *HA3*, target #2 | Fwd LP: 5′-GCTACGTAGACTAGACGTTCTGGAAGCATTCCCAATGACA-3′ |
| | | Rev: 5′-GTACATTYCGCATCCCTGTTG-3′ |
| | *HA3*, target #3 | Fwd: 5′-AACTGACTCAGAAATGAACAAACTGT-3′ |
| | | Rev LP: 5′-GCTACGTAGACTAGACGTTCTGAAACAACCATTGCCCATATC-3′ |
| | *HA3*, target #4 | Fwd: 5′-GGTGTTGAGCTGAAGTCAGGA-3′ |
| | | Rev LP: 5′-GCTACGTAGACTAGACGTTCGCAGGCCCACATGATGAAC-3′ |
| | | UP: 5′-FAM-CCCTATCGCTACGTAGACTAGACGTTC-3′ |
| | | UAP: 5′-TAGTCTACGTAGCGATAGGG-BHQ1-3′ |

(*table continues*)

**Table 1** (*continued*)

| Target organism | Target gene | Primer, probe, or antiprobe sequence |
|---|---|---|
| Influenza A | A/Hong Kong/483/97 | Fwd LP: 5′-GCTACGTAGACTAGACGTTCTGCCGGAATGGTCTTACATAGTG-3′ |
| | *HA5*, target #1 | Rev: 5′-CCCTGGGTAACAGAGGTCATTG-3′ |
| | *HA5*, target #2 | Fwd LP: 5′-GCTACGTAGACTAGACGTTCGTATGCCATTCCACAACATACACC-3′ |
| | | Rev: 5′-GTCGCAAGGACTAATCTGTTTGA-3′ |
| | *HA5*, target #3 | Fwd LP: 5′-GCTACGTAGACTAGACGTTCGAGGAAATAAGTGGAGTAAAATTGGA-3′ |
| | | Rev: 5′-CCATGATTGCCAGTGCTAGG-3′ |
| | | UP: 5′-FAM-CCCTATCGCTACGTAGACTAGACGTTC-3′ |
| | | UAP: 5′-TAGTCTACGTAGCGATAGGG-BHQ1-3′ |
| Influenza A | A/New York/18/2009 | Fwd: 5′-CTTCTAACCGAGGTCGAAACGTA-3′ |
| | *M1* | Rev. ZIPR P: 5′-FAM-GCTTTGAGGGGGCCTGA-3′ |
| | | ZIPR AP: 5′-TCAG**C**CCCCCTCAAAGC-BHQ1-3′ |
| Influenza A | A/California/4/2009 | Fwd: 5′-TGTTAACATCAGCAACACCAACT-3′ |
| | *NA3* | Rev. HUP: 5′-CAL Fluor Red 610-CGTTAACGCCTAAGAGTAGCTAATTTCA-CGGAAACCACTGA-3′ |
| | | HUAP: 5′-CTACTCTTAGGCGTTAACG-BHQ2-3′ |
| Influenza B | B/Ohio/01/05 | Fwd. ZIPR P: 5′-CAL Fluor Red 610-CCCAATTTGGTCAAGAGCAC-3′ |
| | *NS1* | ZIPR AP: 5′-GTGCT**GA**TGACCAAATTGGG-BHQ2-3′ |
| | | Rev: 5′-CTAATTGTCTCCCTCTTCTGGTGA-3′ |
| MTB | *16S rRNA* | Fwd: 5′-GGGATAAGCCTGGGAAACTG-3′ |
| | | Rev: 5′-ACCCCACCAACAAGCTGATA-3′ |
| | | TaqMan P: 5′-FAM-CATGTCTTGTGGTGGAAAGC-BHQ1-3′ |
| MTB | *16S rRNA* | Fwd Flip AP: 5′-BHQ1-AAGACATGCATCCCGTGGT-S9-GGGATAAGCCTGG-GAAACTG-3′ |
| | | Flip P: 5′-TAGGACCACGGGATGCATGTCTT-FAM-3′ |
| | | Rev: 5′-ACCCCACCAACAAGCTGATA-3′ |
| MTB | *inhA* | Fwd: 5′-GCTCGTGGACATACCGATTT-3′ |
| | | Rev. G-Force P: 5′-FAM-CCCCTCCA-S18-AGGAGGGGGTCCGGTAACCAGG-ACTGAAC-3′ |
| | | iDDS P: 5′-CAL Fluor Red 610-GGCGAGACG**T**TAGGTT**A**TCGGGG-Phos-3′ |
| | | iDDS AP: 5′-CCCCGACAACCTATCGTCTCG**G**C-BHQ2-3′ |
| MTB | *katG* | Fwd: 5′-GGGCTGGAAGAGCTCGTAT-3′ |
| | | Rev: 5′-GAGAAGCAGTCGAGGGTGAG-3′ |
| | | M1 iDDS P: 5′-CAL Fluor Red 610-CGATCACCACCGGCA-Phos-3′ |
| | | M1 iDDS AP: 5′-TGCCGGTGGTGA**C**CG-BHQ2-3′ |
| | | M2 iDDS P: 5′-CAL Fluor Red 610-CGCGATCAC**G**AACGGCA-Phos-3′ |
| | | M2 iDDS AP: 5′-TG**A**CGTTGGTGATCGCG-BHQ2-3′ |

Nucleotides in bold text reflect intentional mismatches in probes or antiprobes, where indicated and + represents a locked nucleic acid after the "+" sign. AP, antiprobe; BHQ, Black Hole Quencher; HUAP, Half-Universal antiprobe; HUP, Half-Universal probe; iDDS, internal DNA Detection Switch; K, nonstandard nucleotide, G or T; LP, linker primer; M1, *katG* mutant #1; M2, *katG* mutant #2; MGB, minor groove binder; NFQ, nonfluorescent quencher; P, probe; Phos, 3′ phosphate group to block extension; R, nonstandard nucleotide, A or G; S3, 3-carbon spacer; S9, triethylene glycol spacer; S18, 18-atom hexa-ethyleneglycol spacer; UAP, Universal antiprobe; UP, Universal probe; Y, nonstandard nucleotide, C or T.

needed to develop an effective probe, and then consistent temperature and hybridization conditions are essential for accurate performance.

Here we present seven novel DNA Detection Switch (DDS) probe systems that overcome the difficulties of single-base discrimination with dual-labeled probes, or that deliver versatile, low-cost solutions for qPCR. These seven systems were invented by D.A.S. and are patented or patent pending in the United States, Canada, Europe, and China. DDS probes employ the interaction of two labeled polynucleotide components, a probe, and an antiprobe, wherein the probe binds preferentially to its intended target, turning on signaling, while it dissociates from binding to a nearly complementary antiprobe that otherwise turns off signaling. Typically, the probe component is 5′ labeled with a fluorescent compound, and the antiprobe is 3′ labeled with a quencher compound, although such labeling can be reversed. This general signaling mechanism is termed a DDS. To achieve high-specificity detection, the DDS probe was designed to fully match the target sequence, and the antiprobe is made complementary to the probe except for a carefully placed nonterminal mismatch. The thermodynamics of this design enable exacting target detection because the closely competitive antiprobes that are provided in excess will bind any free-floating probes, quenching their fluorophores, and thereby preventing incorrect or false-positive detection. For targets in which single-base discrimination is not

essential, sensitive and inexpensive detection can be achieved with other DDS probes that use generic components. The designs of the seven DDS probe systems are described subsequently, along with representative applications.

## Materials and Methods

### Primer and Probe Synthesis

Primers and labeled DDS probe components were synthesized by Biosearch Technologies, Inc. (Petaluma, CA) or Integrated DNA Technologies, Inc. (Coralville, IA). Ultramer templates (approximately 120 bases long) were synthesized by Integrated DNA Technologies. Probes were labeled with 5-carboxyfluorescein (FAM), 6-carboxy-2′,4,4′,5′,7,7′-hexachlorofluorescein (HEX), CAL Fluor Red 610 [an equivalent of carboxy-X-rhodamine (ROX)], or Quasar 670 (Cy5 equivalent), and antiprobes were labeled with Black Hole Quencher 1 or 2. With regard to the design of each probe, antiprobe pairing was facilitated by sequence analysis and simulated hybridization testing using the online NUPACK (version 3.0.4, California Institute of Technology, Pasadena, CA) and DINAMelt Web Server (UNAFold version 3.9, Rensselaer Polytechnic Institute, State University of NY at Albany, Troy, NY) programs.[6,7] Customized TaqMan assays were obtained through Applied Biosystems (Carlsbad, CA). Primer, probe, and antiprobe sequences are listed in Table 1.

### Real-Time PCR Studies

For qPCR testing, we typically used the following conditions: 200 nmol/L of the fluorescent probe, 400 nmol/L of the quencher-labeled antiprobe, and 200 nmol/L of any other primer(s). In Universal probe assays, the concentration of linker primer used in the first-step reaction was 20 nmol/L, and Universal probe and antiprobe concentrations were 200 and 400 nmol/L, respectively. We typically used 10 ng of viral cDNA or 1000 to 10,000 copies of ultramer template per reaction. qPCR reactions were performed in 25-μL volumes containing 12.5 μL of 2X HotStart-IT Probe qPCR Master Mix (Affymetrix, Inc., Santa Clara, CA), the indicated template, primer, probe, and/or antiprobe concentrations, and additional $MgCl_2$ and dNTPs (added at final concentrations of 5 and 0.1 mmol/L, respectively). Typical thermal cycling conditions are 95°C, 5 minutes, and then 40 cycles of either two-step PCR (denaturation at 95°C for 15 seconds, and annealing/extension at 58°C for 30 to 60 seconds), or three-step PCR (denaturation at 95°C, 15 seconds; annealing at 58°C, 45 seconds; and extension at 72°C, 45 seconds).

### Test Sample Acquisition

Viral RNA from influenza A strains A/Hong Kong/483/97, A/Vietnam/1203/04, A/Vietnam/Hanoi/30408/05, A/California/

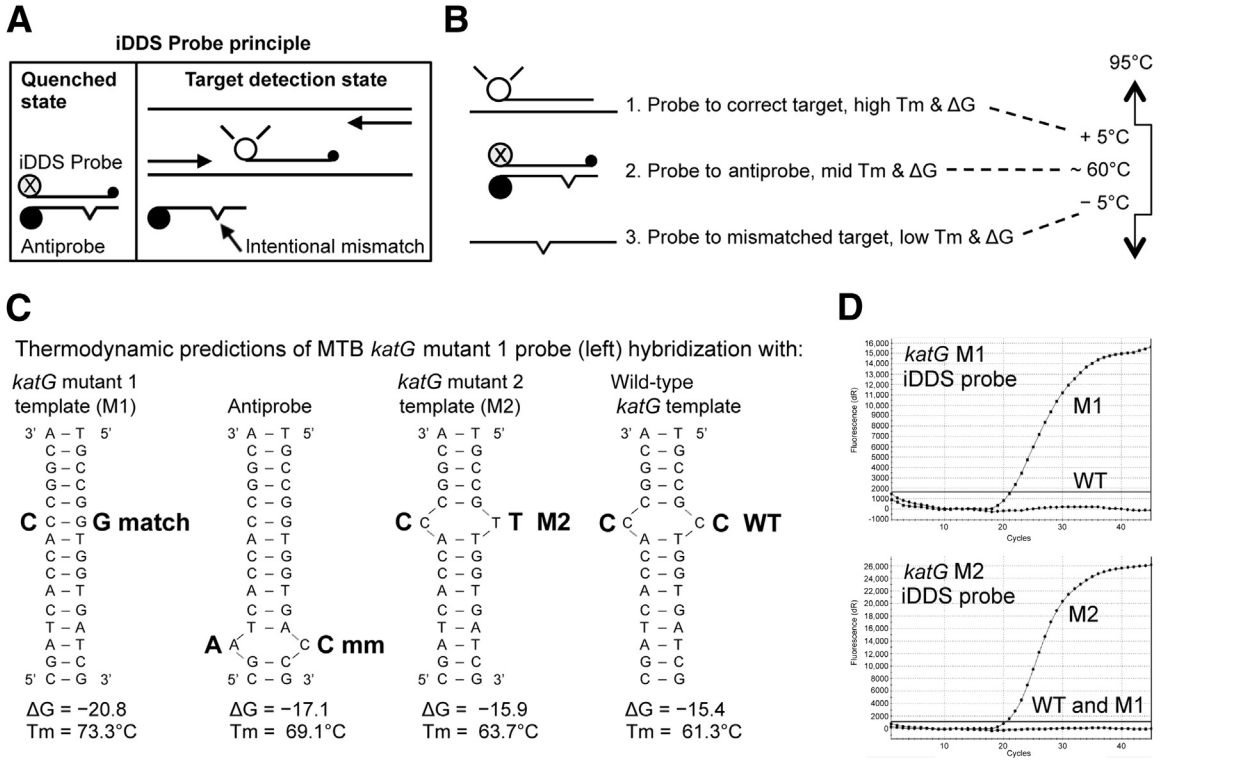


**Figure 1** The iDDS probe system. **A** and **B:** iDDS probe/antiprobe design favors probe binding to (in order of decreasing affinity): i) the correct target, ii) the antiprobe, and iii) a mismatched target. The fluorophore and quencher are indicated with **white** and **black circles**, respectively. Fluor-quencher alignment minimizes background fluorescence to increase the signal/noise ratio.[9–11] **C:** Predicted thermodynamics[6,7] of an MTB *katG* mutant 1 (M1) probe hybridizing to the M1 target, an antiprobe, an alternate mutant (M2), and WT *katG*. These $T_m$ levels run high relative to other common on-line programs. **D:** Single-base discrimination with iDDS probes for two MTB *katG* mutants.

04/2009, A/Solomon Islands/03/2006, and A/New York/18/2009 were gifts from Dr. Ruben Donis [Centers for Disease Control and Prevention (CDC), Atlanta, GA]. RNA from influenza B/Ohio/01/05 was a gift from Dr. Mark Tompkins (University of Georgia, Athens, GA). Viral RNA was reverse-transcribed using random hexamers and the High-Capacity cDNA Reverse Transcription Kit (purchased from Applied Biosystems). *Escherichia coli* samples were gifts from Dr. Michael Vickery (BioGX, Birmingham, AL). Samples of lung cancer DNA with known *EGFR* mutations were gifts from Drs. Charles E. Hill and Michael Rossi (Emory University, Atlanta, GA) and Dr. Mark Bouzyk (AKESOgen, Inc., Norcross, GA). Various *Mycobacterium tuberculosis* (MTB) samples were gifts from Drs. Thomas Shinnick, Wenming Zhu, and James Posey (CDC). A plasmid encoding the full-length HIV-1 NL4-3 molecular clone was obtained at no charge from the AIDS Research and Reference Reagent Program, Division of AIDS, National Institute of Allergy and Infectious Diseases, National Institutes of Health (Rockville, MD), from Dr. Malcolm Martin.[8] Hepatitis B DNA derived from hepatitis $B^+$ human serum or plasma samples was purchased from BBI Diagnostics Inc. (Bridgewater, MA). Synthetic ultramers were used for the MTB and EGFR studies discussed.

## Results

### Internal Probes: iDDS, MacMan, and Flip Probes

The DDS probe systems described here consist of three internal probe systems [internal DDS (iDDS), MacMan, and

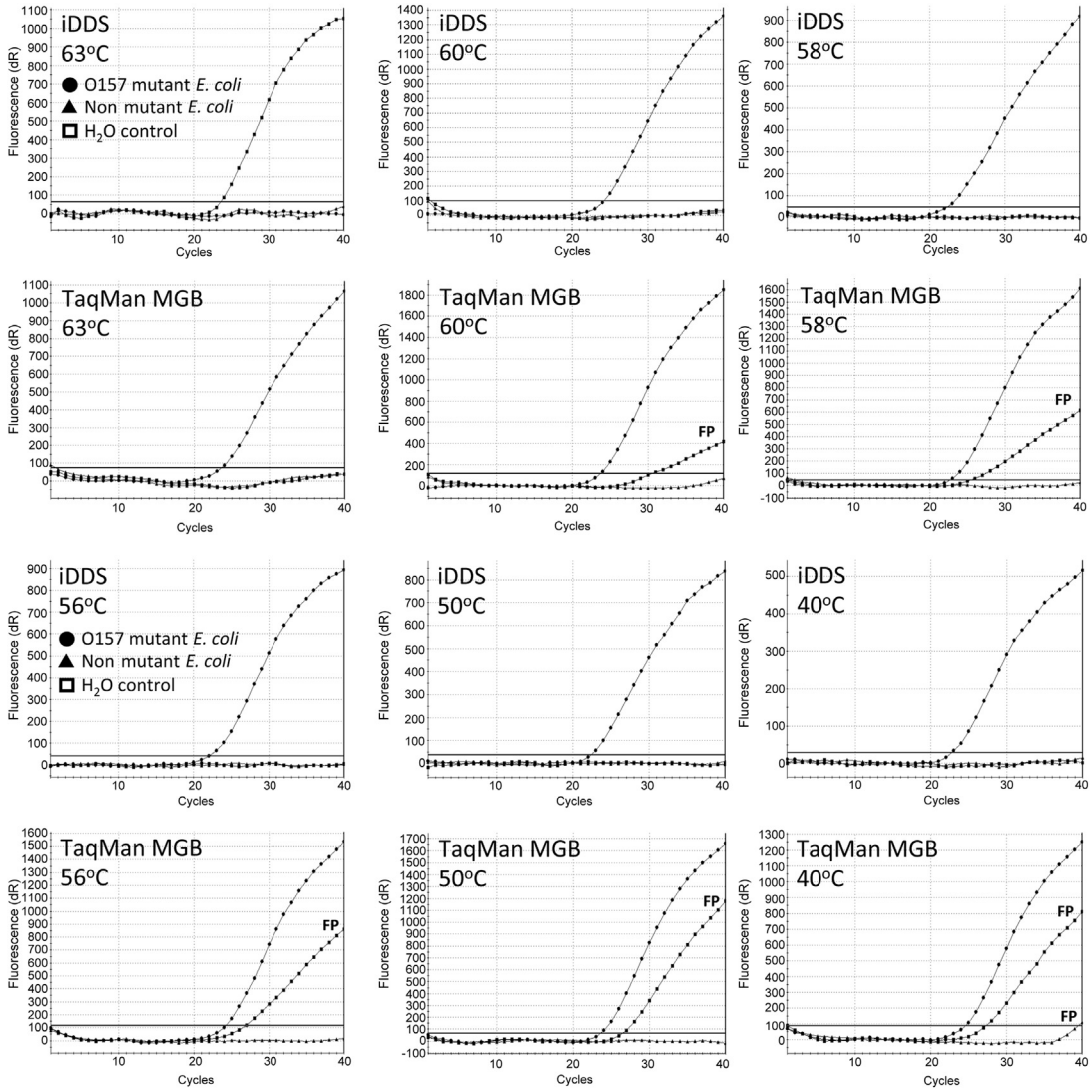


**Figure 2** Performance of iDDS and TaqMan MGB probes in detecting a diagnostic SNP mutant of O157:H7 *E. coli* as a function of annealing temperature. Each graph depicts amplification plots with the mutant *E. coli* template, the WT *E. coli* template, and a water control, with the annealing temperature during qPCR varying from 63°C to 40°C. The TaqMan minor groove binder (MGB) probe shows increasingly obvious false-positive (FP) curves with the WT template as the annealing temperature decreases, and finally shows false-positives with a water control. The iDDS probe demonstrates effective and exclusive detection of the pathogenic *E. coli* SNP variant at all annealing temperatures from 63°C to 40°C.

Flip] and four primer–probe systems (ZIPR, Universal, Half-Universal, and G-Force). Each system will be described sequentially.

The iDDS probe system comprises two equal-length oligonucleotides that interact together: a 5′ fluor-labeled probe that is complementary to the target sequence, and a 3′ quencher-labeled antiprobe that is complementary to the probe except for an intentionally mismatched base (Figure 1, A and B). The 3′ end of the probe is blocked to prevent extension. The target site for the probe is internal to a pair of flanking primers. The iDDS probe structure imparts three distinct levels of thermodynamic binding affinity during the transition from denaturation to annealing: level 1, strong binding [high $T_m$ and low Gibbs free energy ($\Delta G$)] between the probe and a matching target; level 2, intermediate binding between the probe and antiprobe; and level 3, low binding between the probe and a mismatched target differing by a single base. To work effectively, the probe sequence and the position and type of antiprobe mismatch are carefully engineered to achieve $T_m$ and $\Delta G$ differentials of about 5.2°C and about 2.3 kcal/mol, respectively, between each of the three thermodynamic binding levels. The antiprobe therefore provides both a signaling switch and a unique error-checking function that blocks probe binding to incorrect targets even when annealing temperatures are suboptimal. As a result, iDDS probes achieve and maintain single-base discrimination over a wide temperature range. Figure 1B illustrates how the hybridization/annealing step window can shift up or down and still maintain the three affinity levels described earlier such that, during qPCR, the probe binds first to the correct target and then to the antiprobe, and does not bind to an incorrect target at essentially any annealing temperature. Figure 1, C and D illustrates these thermodynamic relationships and the results thereof, with an iDDS probe and antiprobe that detect a point mutation in the MTB catalase-peroxidase gene (*katG*, which confers isoniazid drug resistance)[12,13] and that discriminate between that mutation and an alternate resistance mutation and the wild-type (WT) sequence. Note the $T_m$ and $\Delta G$ differentials between probe-to-target binding, probe–to-antiprobe binding, and probe binding to the incorrect target.

Next, we studied the wide temperature range over which iDDS probes can deliver single-base discrimination. Figure 2 provides an example of this performance by comparing an iDDS probe targeting the +93 SNP in the *uidA* gene of highly pathogenic *E. coli* O157:H7 to the performance of a TaqMan minor groove binder (MGB) probe, designed and recommended by the US Food and Drug Administration (FDA),[14] which targets the same SNP variant. (MGB is an expensive molecular enhancement that enables shorter and more base-specific probes.) The +93 SNP is highly conserved in O157:H7 and O157:H$^-$ strains that produce Shiga toxins, and serves as an accurate identification marker for these severe pathogens.[15] Note that the iDDS probe was designed to run at an annealing temperature of 58°C, whereas the TaqMan MGB probe was designed for a 63°C annealing step. Using the concentrations and PCR conditions recommended by the FDA for the TaqMan MGB probe for O157-H7 *E. coli*,[14] we tested both probes over a series of annealing temperatures ranging from 63°C to 40°C. Note that as the annealing temperature decreases, the TaqMan MGB probe shows a steady increase in false-positive curves with the nonpathogenic *E. coli* template and eventually even with a water control. In contrast, the iDDS probe provides consistent single-base specificity using the same templates and annealing temperatures, making iDDS probes suitable for multiplexing the detection of two or more targets that require single-base discrimination. This capacity is generally not possible with the TaqMan MGB probes.[16]

MacMan probes are constructed with a fluor-labeled probe segment and a generic tail that recruits a matching generic antiprobe with quencher labeling (Figure 3A). The generic sequences lack significant homology with known genomes. During amplification, the probe–antiprobe complex hybridizes to the target region, separating the labeled ends and generating a fluorescent signal. Otherwise, the probe randomly coils, bringing the labeled ends together and turning off detection. Thus, MacMan and TaqMan probe detection occurs via similar mechanisms, although MacMan assays offer a cost advantage because the same generic antiprobe can be used with multiple target-specific probes. A MacMan probe specific for the hepatitis B *S* gene did not detect unrelated HIV-1 or MTB templates (Figure 3B) and showed detection similar to

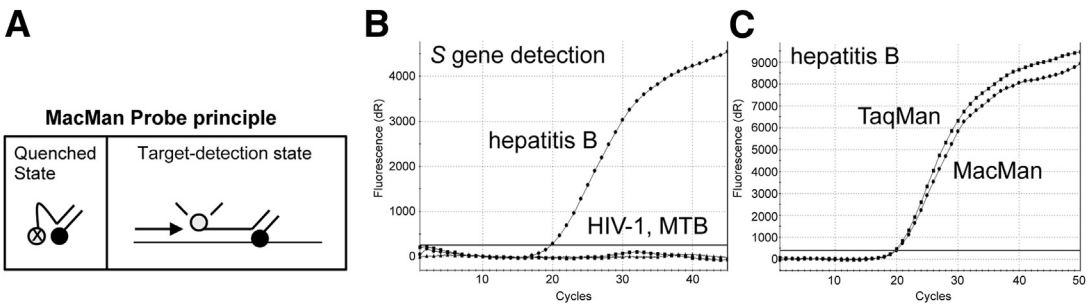


**Figure 3** MacMan probes. **A:** In the absence of target, free-floating MacMan probes are quenched by generic antiprobes that bind generic 3′ tails. Target detection occurs during qPCR as the MacMan probe anneals to the template, separating the probe from the quencher. **B:** MacMan probe detection of the *S* gene of hepatitis B virus DNA (BBI Diagnostics) versus two negative controls (HIV-1 pNL4-3 plasmid and an MTB ultramer template). **C:** Comparison of detection of the hepatitis *S* gene with MacMan versus TaqMan probes for the same target sequence.

that with a TaqMan assay against the same sequence (Figure 3C).

The Flip probe system comprises two components: a 3′ fluor-labeled probe component and a 5′ quencher-labeled antiprobe component that is joined via an S9 spacer (triethylene glycol) to a 3′ primer sequence (Figure 4A). The probe and antiprobe sequences are complementary, except the 5′ end of Flip probes can be made several bases longer than the antiprobe to favor detection. The spacer prevents copying of the antiprobe during PCR. During the annealing step, the probe preferentially flips forward and binds to the targeted DNA sequence between the primer sites, thereby leaving the antiprobe behind and releasing signaling. Although the TaqMan and Flip probes were both effective in detecting the *16S* gene of MTB (Figure 4, B and C), the behavior of one primer was kinetically altered by the Flip probe system so that the amplification curves generated were linear rather than sigmoidal in shape. Consequently, Flip probes enabled true quantitative end point detection similar to the benefit of linear-after−the-exponential PCR (Figure 4D).[17] Note that the fluorescence levels at the end point are proportionate to the cycle threshold values as well as to the starting copy number ($R^2 = 0.985$). Flip probes thus offer both high stringency and end point detection in situations in which a qPCR instrument is not available, such as in many point-of-care facilities.

## Primer-Probes: ZIPR, Universal, Half-Universal, and G-Force Probes

Our DDS primer−probe systems comprise fluorescently tagged primers that drive amplification and that directly label all amplicons for maximum fluorescence. ZIPR primer-probes have a probe−antiprobe structural design (Figure 5A) that is almost the same as that of iDDS probes (Figure 1, A and B), except that the 3′ ends of ZIPR probes are not blocked and they serve as primer probes, not as internal probes. With this design, the antiprobe still improves specificity by inhibiting off-target detection. Figure 5, B and C show ZIPR probes that distinguish homologous sites in the influenza A *M1* gene or the influenza B *NS1* gene. ZIPR probes can also be combined with iDDS probes for two-color detection of each amplicon (Figure 5D). In such applications, the iDDS probe typically targets a specific mutation of interest, whereas the ZIPR probe serves as a reference to confirm the presence and relative quantity of the gene. This approach was used to determine the presence or absence of variably sized deletion mutations that commonly occur in codons 746 to 753 of exon 19 (d-19) of *EGFR* in patients with non-small-cell lung carcinoma.[18] Rather than designing multiple iDDS probes to detect all possible d-19 mutants, a simple one-tube assay was developed using a ROX-labeled ZIPR probe and a FAM-labeled iDDS probe that detects two sites in the same amplicon (Figure 5D). The reference ZIPR probe detects all amplicons of *EGFR* equally, whether WT or with a deletion mutation. However, the iDDS probe only detects and signals whether the full WT sequence is present at the deletion site. Therefore, WT templates provide

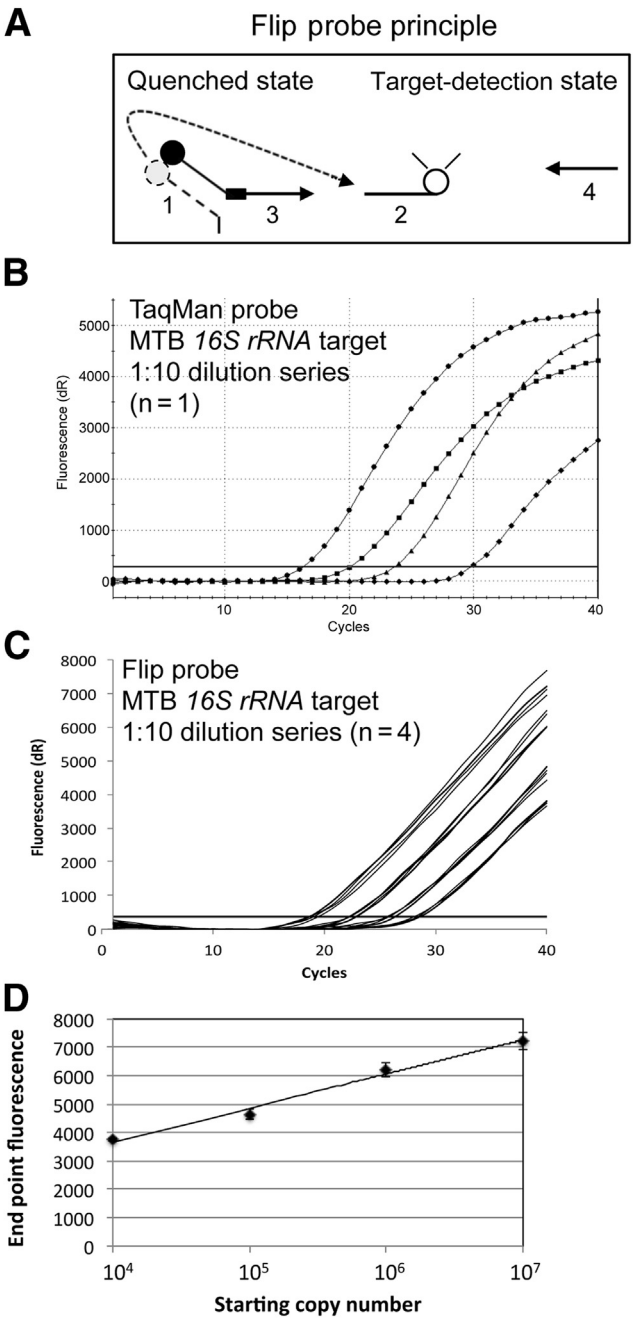


**Figure 4** Flip probes. **A:** In the quenched state, a Flip probe binds to a quencher-labeled antiprobe segment that is joined to a primer. The probe sequence (**dashed line**) is several bases longer than is the antiprobe sequence. The 5′ antiprobe sequence is structurally connected to the 3′ primer sequence by an S9 spacer (triethylene glycol, **black box**). The spacer prevents copying of the antiprobe sequence during qPCR. Numbering in the diagram reflects: i) probe bound to antiprobe, ii) probe bound to target, iii) primer linked to antiprobe, and iv) the second primer. **B** and **C:** Comparison of the TaqMan and Flip probes in detecting the MTB *16S* gene, using MTB genomic DNA that was serially diluted from $10^7$ to $10^4$ copies per reaction. Since TaqMan curves can variably converge at the end point, cycle threshold values must be detected to determine target quantity. In contrast, Flip probe curves are linear so that end point fluorescence also reflects relative target frequency. Linear regression analysis of the MTB samples tested in **C** supports that end point fluorescence at 40 cycles correlates with copy number, and thus, quantitative end point detection may be achieved (**D**). $R^2 = 0.985$, based on four curves per dilution in **C**.

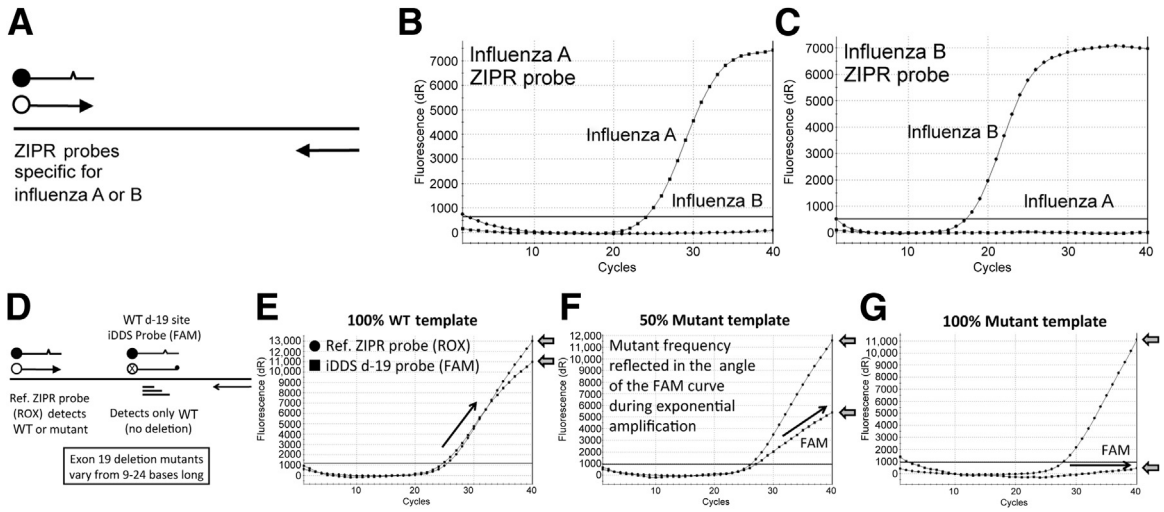


**Figure 5** ZIPR probes. **A:** When ZIPR probes incorporate into PCR products, antiprobe binding is prevented and fluorescence signaling is enabled. ZIPR probes label all amplicons with high sensitivity, and antiprobe intervention favors on-target detection. Discriminating influenza strains using ZIPR probes specific for influenza A/New York/18/2009 *M1* (**B**) or influenza B/Ohio/01/05 *NS1* (**C**) transcripts. **D:** Strategy for detecting *EGFR* d-19 mutants. The reference ZIPR probe targets a conserved sequence upstream of the *EGFR* d-19 site, allowing it to detect both WT and deletion mutants with equal efficacy. In contrast, the FAM-labeled iDDS probe detects only the WT *EGFR* sequence, since all known d-19 mutations (9 to 24 base pairs) disrupt probe binding. Real-time PCR curves observed with samples containing 100% WT template (**E**), 50%/50% WT/mutant template (**F**), or 100% mutant template (**G**). d-19 Mutant frequencies are reflected by the angle of the FAM curve relative to the ROX-labeled reference curve.

two positive ROX/FAM curves (Figure 5E), whereas 100% mutant templates provide only an amplicon-positive ROX curve and a flat FAM curve (Figure 5G). With this method, the relative angle of the FAM curve to the ROX curve is proportional to the frequency of d-19 mutants present in the sample (Figure 5F).

Universal and Half−Universal-primer probes are further variations of DDS technology involving generic probe and antiprobe components. With Universal probes, detection occurs in two stages (Figure 6A). In the first cycle, a linker primer is used to copy and extend the target region with a generic sequence. In subsequent cycles, copies containing the appended sequence serve as a target sequence for the Universal primer−probe. The Universal probe takes over amplification quickly because the linker primer is provided at a lower concentration (20 versus 200 nmol/L). Detection occurs when a Universal probe is incorporated into an amplicon, separating the labeled probe from the generic antiprobe. Because of their generic sequences, Universal probes and antiprobes, prepared in bulk, may be used to detect a new target or a series of targets at basically the cost of the linker primers needed (<$10 each). This strategy can be advantageous for screening multiple target sites to develop an effective assay. Figure 6C shows a Universal probe that discriminates the 2009 pandemic influenza A H1N1 strain[19] from the H1N1 strain in prior circulation. Considering the mutability of viral genomes, greater confidence in molecular diagnostics can be achieved by detecting viral sequences at multiple sites to reduce false-negatives and false-positives. This approach was taken using a single Universal probe−antiprobe pair to detect H3N2 and H5N1 influenza A strains at conserved sites within their *HA* genes (Figure 6, B, D, and E). Although some variation in amplitude was observed, cycle threshold numbers were consistent, as would be expected when detecting the same target species with multiple probes.

In contrast to Universal probes, Half-Universal probes do not use a linker primer and they initiate amplification and detection in one step. A Half-Universal probe is composed of a generic tag sequence with a 5′ label that is joined directly to a 3′ target-specific primer sequence (Figure 6F). In the quenched state, a Half-Universal probe hybridizes with a matching generic antiprobe, but fluorescence is liberated when Half-Universal probes are incorporated into qPCR products. Figure 6G shows a Half-Universal probe specific for the 2009 H1N1 pandemic flu that discriminates against older H1N1 and H5N1 strains, and showed earlier, more robust detection compared with that of the official TaqMan assay from the CDC's real-time reverse-transcription PCR swine flu panel,[20] which targets the same sequence region (Figure 6H). The higher signal/noise ratio of Half-Universal probes versus TaqMan probes reflects the facts that all amplicons are labeled and that quenching is more effective because fluors and quenchers are stably aligned. Figure 6I shows multiplex detection of an H1N1 influenza A RNA sample at three sites within the *HA* gene, based on using three Half-Universal probes with different fluorophores and generic sequences. The presence of parallel but not identical curves supports target detection. Similarly, two Half-Universal probes targeting the *HA* and *NA* genes of the 2009 H1N1 pandemic flu clearly distinguished between viral cDNA samples from the 2009 H1N1 strain and the older H1N1 strain (Figure 6J). The same

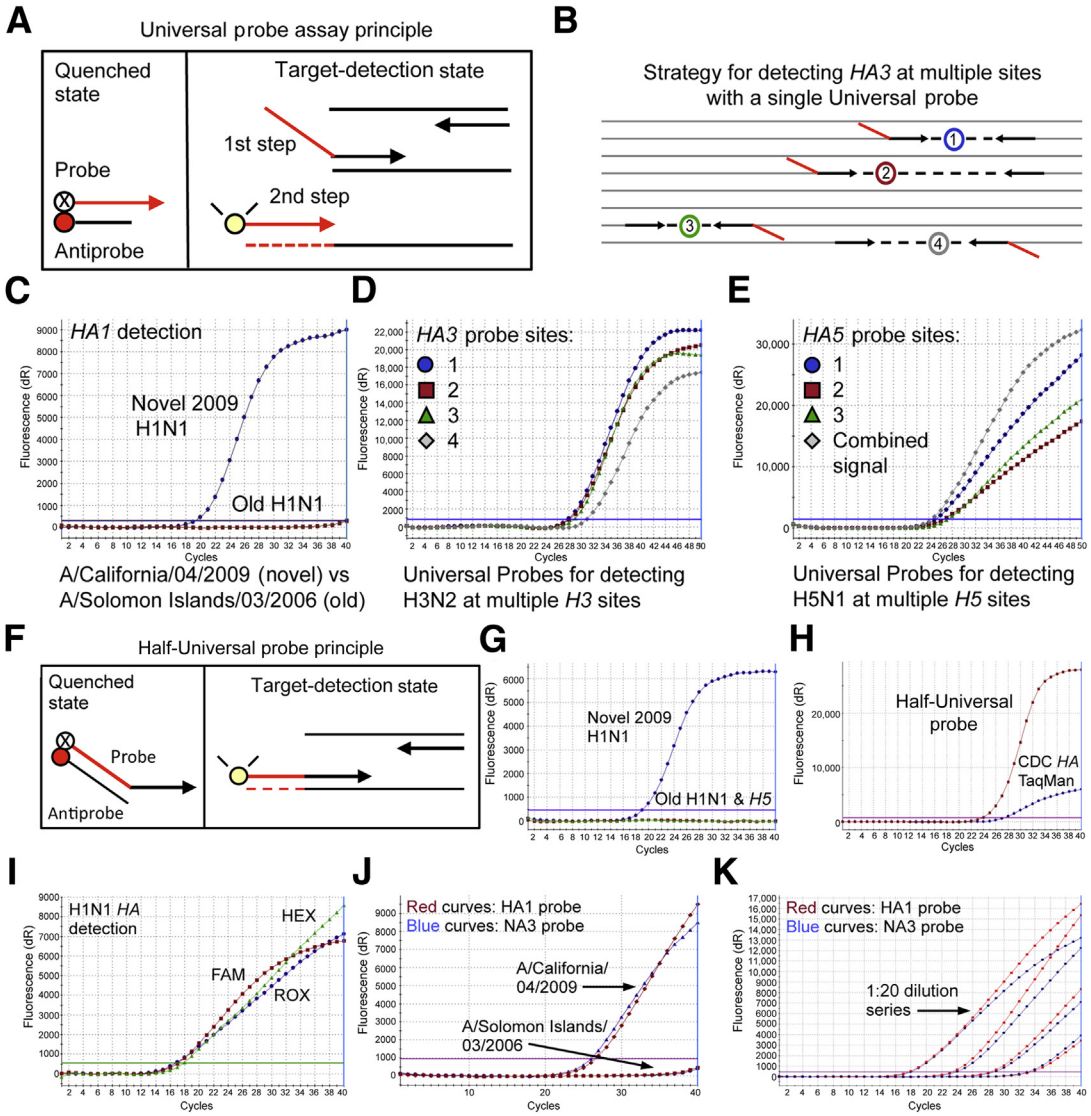


**Figure 6** Universal probes and Half-Universal probes. **A:** Universal probe assays involve two-step detection. The linker primer appends the amplicon with a binding site for the Universal probe (**red**). The linker primer starts amplification in the first cycle, and then the Universal probe takes over and provides signaling. Unincorporated probes are quenched by hybridization with antiprobes. The Universal probe is 7 bases longer than the antiprobe, favoring detection. Schematic representation of an influenza A *HA3* segment and four selected Universal probe sites (**B**), and their use in detecting H3N2 influenza A strain A/Fujian/411/02 (**D**). **C:** Discriminating influenza A/California/04/2009 and A/Solomon Islands/03/2006, using viral cDNA and Universal probes. **E:** Multiplex detection of H5N1 influenza A/Hong Kong/483/97 cDNA at three different *HA5* sites with Universal probes. **F:** Fluorescent Half—Universal-primer probes associate with antiprobes in the absence of target. Amplification separates Half-Universal probes from antiprobes, releasing fluorescence. **G:** A Half-Universal probe targeting H1N1 influenza A/California/4/2009 cDNA discriminated between H1N1 (A/Solomon Islands/03/2006) and H5N1 (A/Hong Kong/483/97) strains. **H:** Half-Universal probe-based detection of the influenza A/California/4/2009 *HA* gene compared with a TaqMan *HA* assay from the CDC real-time reverse-transcription PCR swine flu panel[20]. **I:** Multiplex assays with Half-Universal probes targeting the influenza A/California/4/2009 *HA* gene at three sites. **J:** Multiplex discrimination of influenza A/California/4/2009 and A/Solomon Islands/03/2006 templates using Half-Universal probes. Parallel detection of serially diluted A/California/4/2009 cDNA with the *HA1* and *NA3* Half-Universal probes discussed in **J** and **K**.

probes tested with serial dilutions of the target template produced a series of parallel curves with almost identical cycle threshold values, supporting true-positive detection even with low-frequency templates (Figure 6K).

The G-Force probe system (Figure 7A) consists of a multisegment oligonucleotide with a 5′ fluorescent label, a C-rich segment, an S18 spacer (hexa-ethyleneglycol), a G-rich segment, and a target-specific primer sequence. When the probe is free-floating, the 8-base G-rich and C-rich segments fold together, bringing several Gs near the fluorescent label. The proximal G bases absorb fluorescence by photo-induced electron transfer,[21–23] and thus, the G-rich segment serves as an antiprobe. No quencher is required. As the probe is incorporated into an amplicon, the G-rich segment is copied, folding is prevented, and fluorescent signaling is released. Figure 7, B—D show applications of G-Force probes as low-cost reference probes for detecting an SNP in the human *VKORC1* gene (*rs9923231*) related to

warfarin dosing[24] and the major mutant site of *inhA* that confers isoniazid drug resistance in MTB.[25] The G-Force probe labels the amplicon one color (eg, FAM) irrespective of any WT or mutant sequence between the primers. The iDDS probe selectively detects a mutant or WT sequence using another color (eg, ROX), and the proportion of mutants present will change the angle and amplitude of the iDDS signaling curve, thereby providing a visual index of the mutant frequency.

## Discussion

DDS probes provide effective single-base discrimination, enhanced signaling, and multiplexing. The generic components also enable reduced costs. Three probe systems in particular (iDDS, ZIPR, and Flip) provide high specificity relative to conventional probes (TaqMan, Molecular Beacon) due to the precise and effective role of the antiprobe in blocking off-target detection. The iDDS probe of Figure 2 demonstrates this capacity relative to the FDA-approved TaqMan MGB probe for the same SNP target. The TaqMan MGB probe works specifically at only one optimized annealing temperature (63°C), whereas the iDDS provides similar single-base discrimination over a 23°C range (63°C to 40°C). No other qPCR probe system exhibits this capacity for consistent single-base discrimination over a wide range of annealing temperatures. Moreover, this flexibility eases the design of multiplex iDDS assays because different probes can be run together even if their predicted $T_m$s differ significantly (Figures 5D and 7D).

iDDS and ZIPR probe performance may be predicted by simulated hybridization testing (Figure 1C).[6,7] In general, single-base discrimination is achievable when stepwise changes of about 5°C to 5.5°C in $T_m$ and about 2.2 to 2.7 kcal/mol in ΔG are predicted when going from probe-to-correct target hybridization to probe—to-antiprobe hybridization, and finally to probe-to-off-target hybridization. This process is easily fine-tuned for optimal $T_m$ and ΔG differences by systematic base substitutions in the antiprobe. These thermodynamics thus provide an overall $T_m$ window of 10°C or more between the three affinity levels. In some cases, it is necessary to introduce a mismatch into the probe to achieve the 10°C $T_m$ difference. Such intentional probe mismatches are positioned two bases either upstream or downstream of the targeted mutation, such that probe-to-off-target hybridization is greatly destabilized through the formation of a 3-base hybridization bubble.[7] Differences in $T_m$ resulting from mismatches are position dependent, with internal mismatches being more destabilizing than terminal mismatches.[26] Thus, probes are typically designed with the targeted mutation or SNP located within two or three bases from the probe center, whereas the antiprobe mismatch is positioned three to seven bases from either the 5′ or 3′ end.

While the antiprobe of ZIPR probes increases specificity compared with standard primers or other primer—probe systems (Sunrise, Scorpion probes), they still have a small potential for false-positive results. Nonetheless, they serve as effective reference probes when used in conjunction with iDDS probes. In such cases, the reference probe detects gene/amplicon frequency, and the internal probe detects the relative mutant frequency. With this approach (Figure 5, D—F), we have positively detected the presence of variably sized transforming *EGFR* deletion mutants[27,28] that cannot be detected with single-probe methods. Alternatively, the G-Force probe

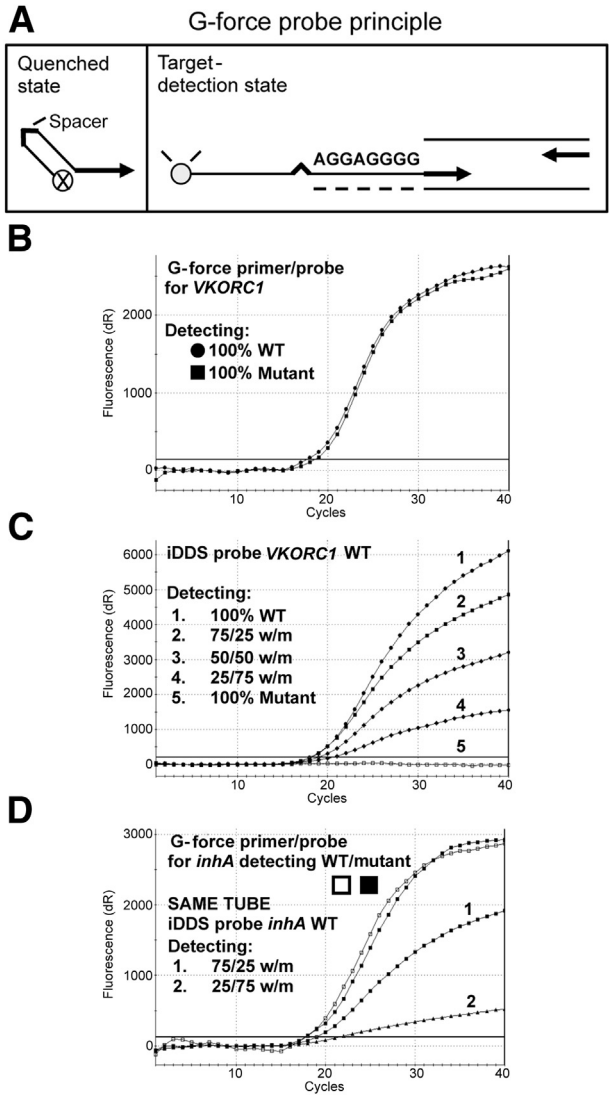


**Figure 7** G-Force probes. **A:** G-Force probes consist of complementary C- and G-rich regions that self-hybridize in the quenched state to juxtapose the fluorophore and the G-rich region, or separate during amplification to activate detection. **B:** A flanking G-Force probe targeting a conserved site in the human *VKORC1* gene shows comparable detection of ultramer templates encoding the WT and SNP variant *rs9923231*[C]. **C:** iDDS probe detection of the WT *VKORC1* template, using mixed WT and SNP variant templates ranging from 100% to 0% WT. **D:** Multiplex detection of the WT MTB *inhA* gene with mixed WT/mutant templates. qPCR was performed using a reference G-Force probe and an iDDS probe targeting the WT sequence at a site that confers isoniazid resistance when mutated. With the 75% WT sample, the iDDS signaling curve drops about 25% relative to the G-Force curve, and with the 25% WT sample, the iDDS curve drops another 50% relative to the G-Force curve, providing semiquantitative mutant frequency analysis. w/m, WT/mutant.

can serve in a capacity similar to that of a low-cost reference probe (Figure 7, B and D).

The DDS probe systems that use generic components (MacMan, Universal, and Half-Universal probes) provide significant cost advantages because the labeled generic components can be made in bulk (Figures 3 and 6). However, these systems also facilitate assay optimization because they lower the cost of testing multiple alternative targets. For example, when developing an assay to detect avian influenza (Figure 6E), primer design programs such as Primer3[29] were inadequate for selecting potential primers that target conserved sites. However, because Universal probes and antiprobes can be used with any linker-extended primer, a shotgun targeting approach could be used to quickly screen 30 potential primer pairs to identify the most efficient sets. Similarly, these low-cost assays enable multitarget diagnostics, an approach that can reduce both false-negatives and false-positives. Because Half-Universal probes use one generic component, they allow only partial cost reduction. However, they also provide quicker one-step detection and have less potential for cross-reaction. G-Force probes also offer cost savings because they obviate a quencher label by exploiting the natural ability of guanines to quench a fluorophore such as FAM.

Collectively, these data illustrate the potential of DDS technologies to provide highly specific and sensitive detection compared with standard qPCR probes. Routine diagnostics may also benefit from the use of lower-cost generic probes and antiprobes for assay optimization or for easy targets. In contrast, the detection of SNPs, somatic mutations, and drug-resistant variants can be better served with iDDS or Flip probes versus the standard probes. We also project the use of iDDS, ZIPR, and Universal probes for validating SNP or gene fusion discoveries from next-generation sequencing or array technologies.[30] Finally, combining primer−probes with iDDS or Flip probes can facilitate the analysis of mutant variants by providing signature profiles that indicate mutant frequency. Further publications will document additional applications for DDS probes as well as clinical validation studies that are currently in progress.

## Acknowledgments

We thank Ruben Donis (Centers for Disease Control and Prevention, Atlanta, GA) and Mark Tompkins (University of Georgia, Athens, GA) for influenza samples; Charles E. Hill and Michael Rossi (Emory University, Atlanta, GA) and Mark Bouzyk (AKESOgen, Inc., Norcross, GA) for DNA extracted from lung cancers with known *EGFR* mutations; and Thomas Shinnick, Wenming Zhu, and James Posey (Centers for Disease Control and Prevention) for MTB samples.

## References

1. Heid CA, Stevens J, Livak KJ, Williams PM: Real time quantitative PCR. Genome Res 1996, 6:986−994
2. Tyagi S, Kramer FR: Molecular beacons: probes that fluoresce upon hybridization. Nat Biotechnol 1996, 14:303−308
3. Bonetta L: Prime time for real-time PCR. Nat Methods 2005, 2:305−312
4. Cheng J, Zhang Y, Li Q: Real-time PCR genotyping using displacing probes. Nucleic Acids Res 2004, 32:e61
5. Zhang DY, Chen SX, Yin P: Optimizing the specificity of nucleic acid hybridization. Nat Chem 2012, 4:208−214
6. Dirks R, Bois JS, Schaeffer J, Winfree E, Pierce NA: Thermodynamic analysis of interacting nucleic acid strands. SIAM Rev 2007, 49:65−88
7. Markham NR, Zuker M: DINAMelt web server for nucleic acid melting prediction. Nucleic Acids Res 2005, 33:W577−W581
8. Adachi A, Gendelman HE, Koenig S, Folks T, Willey R, Rabson A, Martin MA: Production of acquired immunodeficiency syndrome-associated retrovirus in human and nonhuman cells transfected with an infectious molecular clone. J Virol 1986, 59:284−291
9. Didenko VV: DNA probes using fluorescence resonance energy transfer (FRET): designs and applications. Biotechniques 2001, 31: 1106−1116. 1118, 1120-1101
10. Kutyavin IV: New approach to real-time nucleic acids detection: folding polymerase chain reaction amplicons into a secondary structure to improve cleavage of Forster resonance energy transfer probes in 5′-nuclease assays. Nucleic Acids Res 2010, 38:e29
11. Kutyavin IV, Afonina IA, Mills A, Gorn VV, Lukhtanov EA, Belousov ES, Singer MJ, Walburger DK, Lokhov SG, Gall AA, Dempcy R, Reed MW, Meyer RB, Hedgpeth J: 3′-minor groove binder-DNA probes increase sequence specificity at PCR extension temperatures. Nucleic Acids Res 2000, 28:655−661
12. Baker LV, Brown TJ, Maxwell O, Gibson AL, Fang Z, Yates MD, Drobniewski FA: Molecular analysis of isoniazid-resistant Mycobacterium tuberculosis isolates from England and Wales reveals the phylogenetic significance of the ahpC -46A polymorphism. Antimicrob Agents Chemother 2005, 49:1455−1464
13. Lavender C, Globan M, Sievers A, Billman-Jacobe H, Fyfe J: Molecular characterization of isoniazid-resistant Mycobacterium tuberculosis isolates collected in Australia. Antimicrob Agents Chemother 2005, 49: 4068−4074
14. Feng P, Weagant SD, Jinneman K: Diarrheagenic Escherichia coli. In Bacteriological Analytical Manual, ch 4A [Internet]. Copyright AOAC International, 1998-2014. Available at http://www.fda.gov/Food/FoodScienceResearch/LaboratoryMethods/ucm070080.htm, last revised July 2014.
15. Feng P: Identification of Escherichia coli serotype O157:H7 by DNA probe specific for an allele of uid A gene [erratum in: Mol Cell Probes 1993, 7:337]. Mol Cell Probes 1993, 7:151−154
16. Schneider BP, Radovich M, Sledge GW, Robarge JD, Li L, Storniolo AM, Lemler S, Nguyen AT, Hancock BA, Stout M, Skaar T, Flockhart DA: Association of polymorphisms of angiogenesis genes with breast cancer. Breast Cancer Res Treat 2008, 111:157−163
17. Sanchez JA, Pierce KE, Rice JE, Wangh LJ: Linear-after-the-exponential (LATE)-PCR: an advanced method of asymmetric PCR and its uses in quantitative real-time analysis [erratum in: Proc Natl Acad Sci U S A 2009, 106:2083]. Proc Natl Acad Sci U S A 2004, 101: 1933−1938
18. Pao W, Miller V, Zakowski M, Doherty J, Politi K, Sarkaria I, Singh B, Heelan R, Rusch V, Fulton L, Mardis E, Kupfer D, Wilson R, Kris M, Varmus H: EGF receptor gene mutations are common in lung cancers from "never smokers" and are associated with sensitivity of tumors to gefitinib and erlotinib. Proc Natl Acad Sci U S A 2004, 101: 13306−13311
19. Lorusso A, Faaberg KS, Killian ML, Koster L, Vincent AL: One-step real-time RT-PCR for pandemic influenza A virus (H1N1) 2009 matrix gene detection in swine samples. J Virol Methods 2010, 164:83−87
20. Shu B, Wu KH, Emery S, Villanueva J, Johnson R, Guthrie E, Berman L, Warnes C, Barnes N, Klimov A, Lindstrom S: Design and performance of the CDC real-time reverse transcriptase PCR swine flu panel for detection of 2009 A (H1N1) pandemic influenza virus. J Clin Microbiol 2011, 49:2614−2619

21. Crockett AO, Wittwer CT: Fluorescein-labeled oligonucleotides for real-time PCR: using the inherent quenching of deoxyguanosine nucleotides. Anal Biochem 2001, 290:89–97
22. Doose S, Neuweiler H, Sauer M: Fluorescence quenching by photo-induced electron transfer: a reporter for conformational dynamics of macromolecules. Chemphyschem 2009, 10:1389–1398
23. Noble JE, Wang L, Cole KD, Gaigalas AK: The effect of overhanging nucleotides on fluorescence properties of hybridising oligonucleotides labelled with Alexa-488 and FAM fluorophores. Biophys Chem 2005, 113: 255–263
24. Limdi NA, Beasley TM, Crowley MR, Goldstein JA, Rieder MJ, Flockhart DA, Arnett DK, Acton RT, Liu N: VKORC1 polymorphisms, haplotypes and haplotype groups on warfarin dose among African-Americans and European-Americans. Pharmacogenomics 2008, 9:1445–1458
25. Banerjee A, Dubnau E, Quemard A, Balasubramanian V, Um KS, Wilson T, Collins D, de Lisle G, Jacobs WR Jr: inhA, a gene encoding a target for isoniazid and ethionamide in Mycobacterium tuberculosis. Science 1994, 263:227–230
26. Urakawa H, Noble PA, El Fantroussi S, Kelly JJ, Stahl DA: Single-base-pair discrimination of terminal mismatches by using oligonucleotide microarrays and neural network analyses. Appl Environ Microbiol 2002, 68:235–244
27. Kimura H, Kasahara K, Kawaishi M, Kunitoh H, Tamura T, Holloway B, Nishio K: Detection of epidermal growth factor receptor mutations in serum as a predictor of the response to gefitinib in patients with non-small-cell lung cancer. Clin Cancer Res 2006, 12: 3915–3921
28. Ladanyi M, Pao W: Lung adenocarcinoma: guiding EGFR-targeted therapy and beyond. Mod Pathol 2008, 21(Suppl 2):S16–S22
29. Rozen S, Skaletsky H: Primer3 on the WWW for general users and for biologist programmers. Methods Mol Biol 2000, 132:365–386
30. Giacomini CP, Sun S, Varma S, Shain AH, Giacomini MM, Balagtas J, Sweeney RT, Lai E, Del Vecchio CA, Forster AD, Clarke N, Montgomery KD, Zhu S, Wong AJ, van de Rijn M, West RB, Pollack JR: Breakpoint analysis of transcriptional and genomic profiles uncovers novel gene fusions spanning multiple human cancer types. PLoS Genet 2013, 9: e1003464